Acoustic Radiation Force on a Spherical Fluid or Solid Elastic Particle Placed Close to a Fluid or Solid Elastic Half-Space

Thierry Baasch[*] and Jürg Dual

Institute for Mechanical Systems, Swiss Federal Institute of Technology Zurich, 8092 Zurich, Switzerland

The acoustic radiation force acting on a spherical particle placed close to the interface of two infinite half-spaces that is excited by a normally incident traveling wave is investigated using the finite element method (FEM). The medium surrounding the particle is water, whereas different material models are used for the particle itself and the second half-space. Recently, acoustic force spectroscopy has been developed, a technology that uses acoustic forces to measure the mechanical properties of small filaments. If acoustics are used to manipulate particles that are placed very close to an interface then the acoustic interactions between the particle and interface lead to an acoustic interaction force. This interaction force was neglected in previous studies and is included in the total acoustic radiation force obtained by our FEM model. Comparing our results to the primary radiation force that can be obtained using the Gor'kov potential, we found that, for cells (red blood cells or fat cells) immersed in water and placed close to a PMMA, glass, or silicon domain, the magnitude of the acoustic interaction force can exceed 10% of the magnitude of the primary radiation force. In other cases, the acoustic interaction force can be even larger in amplitude and of opposite sign than the primary force.

I. INTRODUCTION

The earliest experimental investigations of the acoustic radiation force acting on particles close to interfaces focused on bubbles, because in this case the acoustic radiation force can be easily observed at small excitation amplitudes. In 1965, Howkins et al. [1] measured the resonant frequency of a bubble near a rigid boundary. In 1981, Shima et al. [2] investigated the interaction between bubbles and solid walls experimentally. More recent experimental investigations by Zhao et al. [3,4] and Payne et al. [5] focused on bubbles and contrast agents attached to walls. Garbin et al. [6] used high-speed imaging to measure the microbubble dynamics near a boundary. Doinikov et al. [7] investigated the scattering of a bubble close to a wall of finite thickness and density both experimentally and theoretically. The early experimental works were accompanied by theoretical investigations. Because of the complexity of the full problem, researchers have devised a number of simplifications, such as neglecting the shape oscillations of the particle, assuming the particle or wall to be perfectly rigid, or a cylindrical shape of the particle, which significantly simplify the problem and allow for analytical solutions [5,8–13]. Doinikov et al. provided analytical calculations for spherical bubbles and contrast agents close to an elastic half-space [14], a fluid layer of

finite density and thickness [15], an elastic wall of finite thickness [16], and two parallel elastic walls [17].

Numerical investigations focused, to our knowledge, either on single isolated particles [18,19] or on particle interactions with rigid walls [11,20,21].

Examples of recent applications that use the acoustic radiation force to manipulate particles and bubbles placed close (at the order of the diameter) to interfaces are the acoustic force spectroscopy [22,23] and acoustic tweezing cytometry [24]. In acoustic force spectroscopy, a micrometer sized bead attached to a channel wall by a biological filament is moved by acoustic forces. The displacement of the bead in combination with the Gor'kov potential [25] used to model the acoustic radiation force then yields the mechanical stiffness of the biological filaments. In this case, the acoustically manipulated beads are placed at a distance comparable to the particle diameter from the channel walls. The use of Gor'kov's potential theory is questionable as it is only valid in the free field far from interfaces.

We numerically investigate the acoustic radiation force acting on a particle placed in water close, i.e., at a distance d of the order of the particle radius a, to a half-space of different material (denoted *domain 2*), while keeping the wavelength λ much larger than the particle radius a. Although, we focus our investigation on wavelengths λ much larger than the particle radius a, this is not a limitation of the technique. Both the particle and half-space

---

*baasch@imes.mavt.ethz.ch

are modeled as elastic solid, inviscid fluid and several ide-alized materials. The inviscid assumption is expected to be a good approximation as long as the gap between the particle and the interface sufficiently exceeds the size of the viscous boundary layer. Special emphasis is put on comparing the acoustic radiation force that acts on a particle placed close to an interface to that acting on a particle in the absence of the second half-space. Thus, we establish when the Gor'kov potential is a good approximation to calculate the acoustic radiation force acting on a particle close to an interface.

II. METHODS

The finite element model (COMSOL Multiphysics 5.4) consists of the particle placed in a water domain separated from domain 2 by the interface at $z = 0$, as sketched in Fig. 1(a). Thedomains are surrounded by a perfectly matched layer to absorb all outgoing radiation, so that our water domain and domain 2 behave approximately like infinite half-spaces. Domain 2 and the particle are modeled as an elastic solid as well as an inviscid fluid. The system is excited by plane waves traveling in the positive z direction. The incident and reflected plane waves propagate in the water domain and the transmitted plane wave propagates in domain 2. Together, these three plane waves constitute the background field. At the particle-water and water-domain 2 interfaces we impose continuity for the stresses and velocities in the normal direction. The complete problem is axially symmetric, which we exploited in our simulations.

In the right panel of the Fig. 1 the "no domain 2" (ND2) setup is shown. The ND2 model consists of the particle and water domain surrounded by a perfectly matched layer
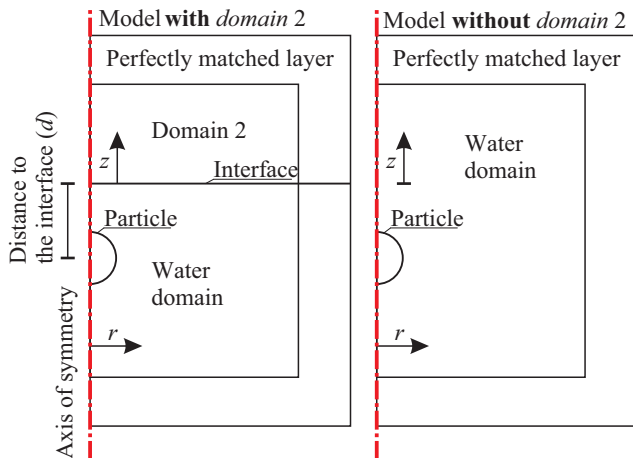

FIG. 1. We use two different setups in our simulations. The model with domain 2 (left) consists of the particle placed in the water domain that is separated from domain 2 by the interface. The model without domain 2 (ND2) is composed of the particle and the water domain only.

without a domain 2. The ND2 model is excited by incident and reflected plane waves, such that the particle experiences the same background field as in the model with domain 2. The ND2 setup is further explained in Sec. II E. In the scattering simulation for the ND2 model, we used the background field as given by Eq. (16). The ND2 model provides free-space reference values for the acoustic radiation force that converge asymptotically to the results obtained from the model with domain 2 when increasing the separation distance between the particle and interface. Although we use the finite element method (FEM) to calculate the acoustic radiation force in the ND2 setup, it is also possible to get an approximate analytical solution; see Sec. II E.

A. Modeling the fluid and solid domains

Assuming an inviscid fluid of density ρ and time harmonic fields with radial frequency ω and time harmonic factor $e^{i\omega t}$, we can model the first-order dynamics using the Helmholtz equation [26] for the (complex-valued) velocity potential ϕ:

$$\partial_j \partial_j \phi + k^2 \phi = 0. \tag{1}$$

Here we used the tensor notation and the Einstein summation convention, shortened the notation for the partial derivative $\partial/\partial x_i$ to ∂_i, and used $k = \omega/c$ to denote the wave number. The (real-valued) velocity v_i and pressure p fields can then be calculated by $v_i = \mathrm{Re}(\partial_i \phi \, e^{i\omega t})$ for $i = 1, 2, 3$ and $p = \mathrm{Re}(-i\rho\omega\phi \, e^{i\omega t})$, respectively.

Assuming linear kinematics and time harmonic fields in the elastic solid domains, the motion of a linear elastic solid can be described by

$$\partial_j \partial_j \phi' + k_p'^2 \phi' = 0, \tag{2}$$

$$\partial_j \partial_j \psi_i' + k_s'^2 \psi_i' = 0 \quad \text{for } i = 1, 2, 3, \tag{3}$$

$$\text{and} \quad \partial_i \psi_i' = 0, \tag{4}$$

where the prime is used to denote the fields and constants in the solid elastic domain that, depending on the setup, can be the particle, domain 2, or both. Note that materials of the particle and domain 2 are not necessarily the same. Here, the respective wave numbers are defined for a constant angular frequency ω by $k_p' := \omega/c_p'$ and $k_s' := \omega/c_s'$, where c_p' and c_s' are the primary (P) and secondary (S) wave speeds in the solid. In the solid, the velocity field $\mathbf{v}'$ is derived from the potentials by $\mathbf{v}' = \mathrm{Re}(\nabla\phi' \cdot e^{i\omega t} + \nabla \times \boldsymbol{\psi}' \cdot e^{i\omega t})$. At all interfaces, we impose continuity of normal stresses and normal velocities.

B. Acoustic radiation force

The radiation force acting on a particle in an inviscid fluid is given by [27,28]

$$
F_i = -\left\langle \int_{\partial\Omega} \left[\left(\frac{1}{2} \frac{1}{\rho c^2} p^2 - \frac{\rho}{2} v_j v_j \right) \delta_{ik} + \rho v_k v_i \right] n_k da \right\rangle
$$
$$
\text{for } i = 1, 2, 3, \tag{5}
$$

where the angled brackets denote time averaging $\langle \square \rangle := (1/T) \int_T \square dt$ and the n_k denote the components of the outward pointing normal vector to the fixed surface $\partial\Omega$. It is not necessary that the integration surface $\partial\Omega$ coincides with the particle boundary. Any fixed surface encompassing the particle can be chosen as long as no other singularities are included. Because of the axial symmetry of our setup, the only nonzero component of the acoustic radiation force is in the interface normal direction, i.e., z direction. By convention, a positive force is acting in the positive z direction, as defined in Fig. 1.

C. Acoustic scattering

One typical method to solve for the scattered acoustic fields is to exploit the linearity of the Helmholtz equation. The total field ϕ can then be decomposed into the background ϕ^b and scattered ϕ^s fields:

$$
\phi = \phi^b + \phi^s. \tag{6}
$$

By the superposition principle, if the background field ϕ^b and the scattered field ϕ^s are solutions to the Helmholtz equation then their combination will also be a solution. The addition of the scattered field then allows the total field to fulfill the boundary conditions at the particle surface.

D. Reflection and transmission of normally incident waves at an interface

For the background fields, we consider the reflection and transmission of plane waves at a fluid-fluid or fluid-solid interface under normal incidence. In the case of normal incident waves, no mode conversion occurs at the fluid-solid interface and only a single mode propagates in each domain. For two semi-infinite domains and plane propagating waves, analytical solutions can be found in the literature; see, for example, the books by Blackstock [29] and Ewing [30]. We assume the incident wave to be propagating in the water domain in the positive z direction. Thus, the reflected wave propagates in the water domain and a transmitted wave propagates in domain 2. The velocity potentials of the incident ϕ^{in} and reflected ϕ^{refl} waves

are given by

$$
\phi^{in} = Ae^{-ik_1 z} \tag{7}
$$

$$
\text{and} \quad \phi^{refl} = RAe^{ik_1 z} \tag{8}
$$

in the water domain. In domain 2 the fields are given by

$$
\phi^{tr} = TAe^{-ik_2 z} \tag{9}
$$

for a fluid and by

$$
\phi'^{tr} = T'_1 Ae^{-ik'_p z} \tag{10}
$$

$$
\text{and} \quad \psi'^{tr} = T'_2 Ae^{-ik'_s z} = 0 \tag{11}
$$

for a solid.

The reflection and transmission coefficients (R and T) for normal incidence are found by applying the boundary conditions of continuous normal stresses and velocities at the interface. They are given by

$$
R = \frac{Z_2 - Z}{Z_2 + Z}, \qquad T = T'_1 = \frac{\rho}{\rho_2} \frac{2Z_2}{Z + Z_2}, \tag{12}
$$

where Z, Z_2 and ρ, ρ_2 are the characteristic acoustic impedance and density in the water domain and domain 2, respectively. Note that the characteristic acoustic impedance for a fluid of density ρ and speed of sound c or an elastic solid of density ρ' and primary wave speed c_p is calculated by $Z = \rho c$ or $Z = \rho' c_p$, respectively. In the case of normal incident waves, no mode conversion occurs and T'_2 is zero. However, the field scattered by the particle is not normal incident at the interface. Thus, we observe S waves in our numerical simulations, even if they are not present in the background fields.

E. Analytical approximation of the setup without domain 2

In our numerical simulations, all particle shape modes are included due to the nature of the FEM method. In the limit of a very small particle radius a to wavelength λ ratio, i.e., $ka \ll 1$, the acoustic radiation force acting on the particle can be approximated by considering the monopole and dipole radiations only [25,31,32]. Neglecting viscous and thermal effects, the acoustic radiation force can be calculated using Gor'kov's formula [25] for given

TABLE I.   The properties of the used materials. The particle and domain 2 columns indicate where the material was used inside the particle or domain 2, respectively. The S wave speed for PMMA is calculated using values for the density, Poisson ratio, and P wave speed given by Selfridge [34].

Material	Tag	Density (kg m^{-3})	P wave speed (m s^{-1})	S wave speed (m s^{-1})	Contrast factor (–)	f_0 (–)	f_1 (–)	Particle material	Domain 2 material
Fluid soft	FS	500	500		−5.91	−17	−0.5	Fig. 4	Fig. 5
Fluid hard	FH	2000	3000		0.4917	0.86	0.4	Not applicable	Fig. 5
Solid soft	SS	500	1000	500	−2.1667	−5.8	−0.5	Figs. 5, 6	Fig. 6
Solid hard	SH	2000	5000	3000	0.5045	0.9	0.4	Figs. 5, 6	Fig. 6
Very soft solid 1	T1	50	50	25				Not applicable	Fig. 11
Very soft solid 2	T2	150	180	90				Not applicable	Fig. 11
Very soft solid 3	T3	200	240	120				Not applicable	Fig. 11
Very soft solid 4	T4	400	500	250				Not applicable	Fig. 11
Shear soft solid	T5	500	500	10				Not applicable	Fig. 12
Shear soft solid	T6	500	500	50				Not applicable	Fig. 12
Shear soft solid	T7	500	500	200				Not applicable	Fig. 12
Red blood cell [35,36]	RBC	1100	1600		0.0982	0.2	0.06	Figs. 7, 8, 15	Not applicable
Fat cell [37]	FC	930	1450		−0.075	−0.15	−0.05	Figs. 7, 8, 15	Not applicable
Polystyrene [34]	PS	1050	2400	1150	0.17	0.46	0.03	Figs. 9, 10	Not applicable
PMMA [34]	PMMA	1180	2610	1065				Not applicable	Figs. 7–10,15
Glass [34]	Glass	2240	5640	3280	0.54	0.94	0.54	Figs. 4, 9, 10	Figs. 7–10,15
Silicon [34]	Si	2340	8430	5840				Not applicable	Figs. 7–10,15
Limit soft	LS	0	0	0	−∞			Fig. 3	Fig. 3
Limit hard	LH	∞	∞	∞	5/6			Figs. 3, 11–12	Figs. 3, 4

background pressure p^b and velocity v_i^b, $i = 1, 2, 3$, fields:

$$U = 2\pi a^3 \rho \left(\frac{1}{3} \frac{\langle p^b p^b \rangle}{\rho^2 c^2} f_0 - \frac{1}{2} \langle v_i^b v_i^b \rangle f_1 \right), \quad (13)$$

$$\mathbf{F} = -\nabla U, \quad (14)$$

$$f_0 = 1 - \frac{\kappa_p}{\kappa}, \qquad f_1 = \frac{2(\rho_p - \rho)}{2\rho_p + \rho}. \quad (15)$$

Here we used the monopole f_0 and dipole f_1 scattering coefficients. The monopole and dipole coefficients are functions of the particle density ρ_p and compressibility κ_p, as well as, the water density ρ and compressibility κ.

The background pressure field is chosen to be the sum of an incident and reflected wave,

$$p^b = p_{in}[R \cos(kz + \omega t) + \cos(\omega t - kz)], \quad (16)$$

with the corresponding velocity field

$$v^b = \frac{k p_{in}}{\omega \rho} [\cos(\omega t - kz) - R \cos(kz + \omega t)]. \quad (17)$$

The background pressure given in Eq. (16) is also used as a background field in our scattering simulations using the ND2 model. Using the Gor'kov potential, we arrive at the analytical approximation for the ND2 force in the z
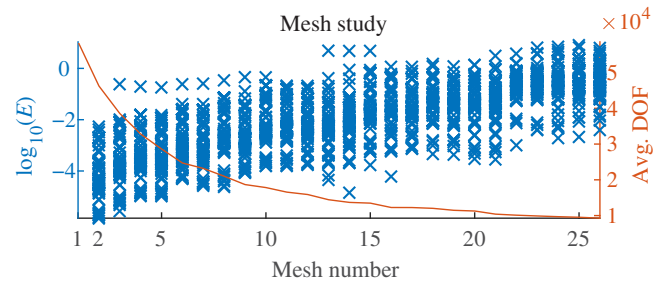

FIG. 2.   The mesh study for our finite element model. The reference mesh is denoted by 1 and has the most degrees of freedom (DOF). Each scatter point represents the performance of a certain mesh number for a given combination of material models. The value of the error percentage (E) results from a comparison with the reference mesh. In our simulations, we use a mesh of quality equal to or better than mesh number 6, for which the resulting error is smaller than one percent with respect to the reference mesh.

TABLE II.   The standard settings used in the simulations.

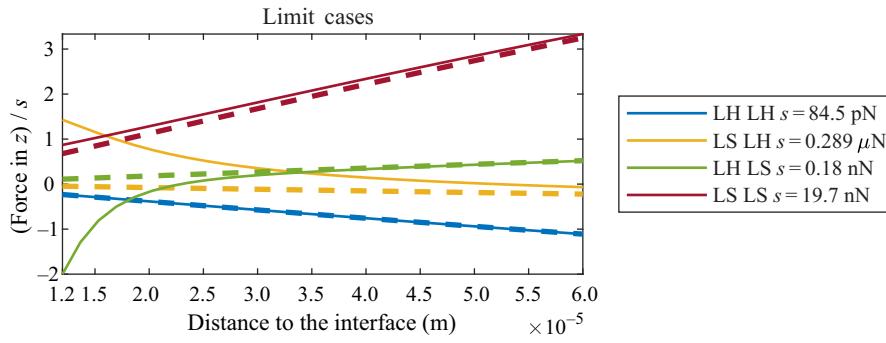| Standard settings	Value
Particle radius	10 μm
Frequency	1 MHz
Water density	1000 kg m^{-3}
Water speed of sound	1500 m s^{-1}
Pressure amplitude of incident wave p_{in}	100 kPa

FIG. 3. The acoustic radiation force for acoustically soft (LS) and hard (LH) limit cases. The solid and dashed lines correspond to the models with and without domain 2, respectively. In the cases of a hard particle with hard domain 2 (LH LH) the interaction force is negligible. For a soft particle placed close to a soft domain 2 (LS LS), the relative difference already exceeds 20%. For a soft particle close to a hard domain 2 (LS LH) and a hard particle close to a soft domain 2 (LH LS), the interaction force even exceeds the primary force.

direction, given by

$$F^{\mathrm{GK}} = 4\pi a^3 \frac{p_{\mathrm{in}}^2}{c^2 \rho} kR\Phi \sin(2kz) \qquad (18)$$

with acoustic contrast factor $\Phi := \frac{1}{3}f_0 + \frac{1}{2}f_1$.

F. Analytical approximation of the setup with a perfectly rigid domain 2

Assuming a perfectly rigid domain 2, i.e., as in the limit hard case of Table II, allows for an analytical approximation of the interaction force, even if the particle is elastic, as long as the particle radius a is much smaller than the acoustic wavelength λ, i.e., $ka \ll 1$. Setting the reflection coefficient R to 1, the background fields reduce to a standing wave (SW). The background pressure field is then given by

$$p^{\mathrm{BSW}} = 2p_{\mathrm{in}} \cos(kz) \cos(\omega t) \qquad (19)$$

with the corresponding velocity field

$$v^{\mathrm{BSW}} = \frac{2kp_{\mathrm{in}}}{\omega \rho} \sin(kz) \sin(\omega t). \qquad (20)$$
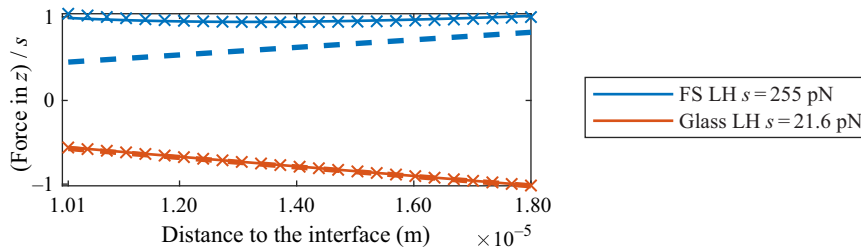
Note that the pressure amplitude of the standing wave is $2p_{\mathrm{in}}$. The ND2 force is given by

$$F^{\mathrm{GKSW}} = 4\pi a^3 \frac{p_{\mathrm{in}}^2}{c^2 \rho} k\Phi \sin(2kz). \qquad (21)$$

The interaction force F^{ISW} for a compressible particle can be derived using the methodology proposed in Ref. [33] and the mirror source concept. For particles at distances d away from the interface and much smaller than the wavelength λ, the results can be expanded in rising orders of the small parameter $\epsilon = dk$, and up to second-order accuracy we have

$$F^{\mathrm{ISW}} = \frac{\pi}{36} \frac{a^6}{d^4} \epsilon^2 \frac{p_{\mathrm{in}}^2}{\rho c^2} (8f_0^2 - 12f_0f_1 + 9f_1^2). \qquad (22)$$

The coefficient $\Psi = (8f_0^2 - 12f_0f_1 + 9f_1^2)$ is the analogue of the acoustic contrast factor for the acoustic force interactions of a particle with a rigid domain 2. The total analytical approximation of the force F^{LH} on a particle at a distance d to a perfectly hard domain 2 is then the sum of the primary force F^{GKSW} and interaction force F^{ISW}, i.e.,

$$F^{\mathrm{LH}} = F^{\mathrm{GKSW}} + F^{\mathrm{ISW}}. \qquad (23)$$

FIG. 4. The acoustic radiation force for a soft fluidic (FS) and a glass particle placed close to a rigid (limit hard) domain 2. The solid and dashed lines correspond to the models with and without domain 2, respectively. The analytical solution F^{LH} is marked by crosses. We observe good agreement between the proposed theory and the numerical results.
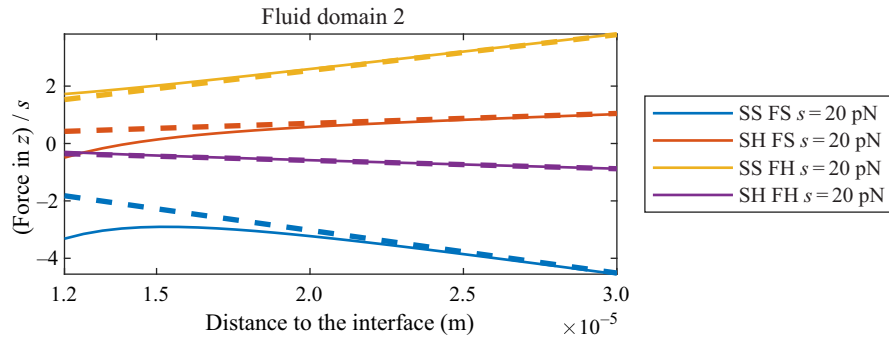
FIG. 5.   The acoustic radiation force for a solid particle placed close to a fluid domain 2. The solid and dashed lines correspond to the models with and without domain 2, respectively. For a soft solid particle placed close to a hard fluid domain 2 (SS FH) and a hard solid particle placed close to a hard fluid domain 2 (SH FH), the relative difference is in the order of 10%. A much stronger interaction force is observed for the SS FS and SH FS combinations. For the hard solid particle with soft fluid domain 2 (SH FS) combination, the interaction force can even induce a sign change.

III. MATERIAL PROPERTIES

The material properties of the used solids and fluids are listed in Table I and our standard settings for the water and acoustic actuation are shown in Table II.

At the interface between the water and the limit soft domain 2 we impose the pressure release boundary condition $\phi = 0$ and at the interface between the limit hard domain 2 and the water we impose the hard wall boundary condition $n_i \partial_i \phi = 0$.

IV. MESH STUDY

If we assume the standard settings from Table II then the acoustic force is uniquely defined for a given material combination, particle distance to the domain 2 d and mesh number m. The mesh number m relates to the number of degrees of freedom, as shown in Fig. 2. We denote the force in this chapter by $F(d, m)$. In our mesh study,

we varied the particle position, material parameters, and mesh quality. For one combination of material parameters in domain 2 and the particle, the distance of the particle center to the interface is varied from 1.2 to 3 times the particle radius in at least ten equidistant steps. This yields a set of acoustic radiation force values per material parameter combination and mesh quality, which we denote by $F = F(d_j, m)$ for $j = 1, \ldots, J > 2$. Let m_1 denote the mesh with number one that has the most degrees of freedom and highest quality. The error percentage of a mesh m_k for a given material combination and a specific model dimension is defined as

$$E(m_k) := \text{mean}_j \left[\left| \frac{F(d_j, m_1) - F(d_j, m_k)}{F(d_j, m_1)} \right| 100 \right]. \quad (24)$$

Many E values can be generated for a given mesh number by simply choosing multiple material model combinations
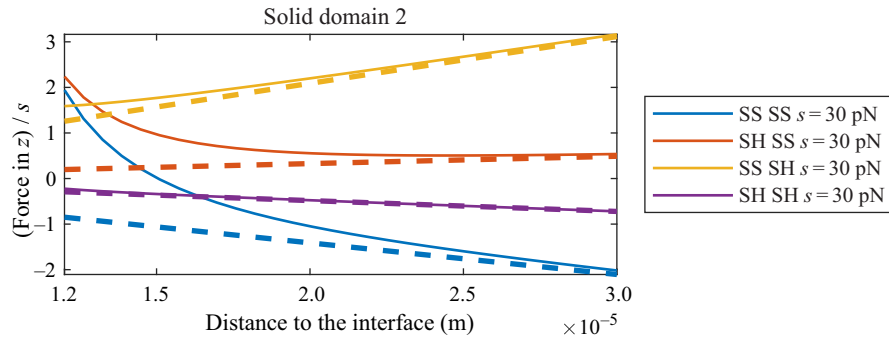

FIG. 6.   The acoustic radiation force for a solid particle placed close to a solid domain 2. The solid and dashed lines correspond to the models with and without domain 2, respectively. For the soft solid particle combined with a hard solid domain 2 (SS SH) and the hard solid particle with a hard solid domain 2 (SH SH) combinations, the relative difference exceeds 20% if the particles are placed close to domain 2. The acoustic interaction force, which we define as the difference between the models with and without domain 2, is large for a soft and hard solid particle placed close to a soft solid domain 2 (SS SS and SH SS). We even observe a sign inversion of the acoustic radiation force between models with and without domain 2 in the case of a soft solid particle placed close to a soft solid domain 2 (SS SS).
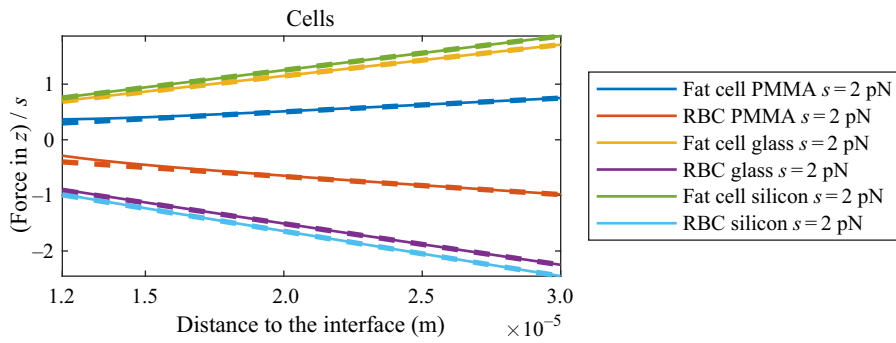
FIG. 7. The acoustic radiation force acting on cells (red blood cells and fat cells) placed close to a PMMA, glass, or silicon domain 2. The solid and dashed lines correspond to the models with and without domain 2, respectively. Our model predicts a relative difference in the order of 1% for cells placed close to a silicon or glass domain 2. If the cells are placed close to a PMMA domain then the relative difference can exceed 20%.

for the particle and domain 2. Each data point in the scatter plot of Fig. 2 corresponds to such an E value. For all our consecutive simulations, we chose a mesh of quality better than or equal to 6 to get a good trade-off between performance and speed. This way the difference in the acoustic radiation force with respect to the reference mesh is below one percent for all models.

V. RESULTS

Before presenting the results, a comment regarding the nomenclature should be made. We abbreviated the labels as shown in Table I. In most of our plots, every label is valid for two data lines inside the plot, one solid line, referring to the simulation with domain 2, and one dashed line, referring to simulations without domain 2. In order to fit all the data on the same scale, we introduced a scaling factor s and we always scaled the data with (solid line) and without (dashed line) domain 2 with the same factor. The material combination is determined by the material inside the particle and the material of domain 2, as the particle is surrounded by inviscid water in all our simulations. The plot line labeling follows the "particle material," "domain material," "scale factor" scheme. For example, FS SH $s = 3$ pN means that the particle material corresponds to the soft fluid, the domain 2 material is the hard elastic solid, and the values need to be multiplied by 3 pN to get the force in Newtons.

To better quantify the differences between the acoustic radiation force calculated using the model without domain 2 (F^{ND2}) and the model with domain 2 (F^{WD2}), we define

the (signed) acoustic interaction force as

$$F^I = F^{\mathrm{WD2}} - F^{\mathrm{ND2}} \tag{25}$$

and the relative difference (R_D) as

$$R_D = \left| \frac{F^I}{F^{\mathrm{ND2}}} \right|. \tag{26}$$

Both of these values are extracted *a posteriori* from the simulations.

A. General considerations

In our setup, the inclusion of domain 2 leads to additional effects with respect to the standard case where the water domain is assumed to be of infinite extent in all directions. The total acoustic radiation force acting on the particle is composed of the primary acoustic radiation force due to the background field, i.e., the no domain 2 force and the acoustic interaction force (F^I) due to the interaction between the particle and the wall. Equation (18) is our analytical approximation to the ND2 force. This force can be positive or negative depending on the material properties of the particle (Φ) and the material properties of domain 2 (R). Note that both Φ and R can be either positive or negative.

The interaction force (F^I) can act in the same or in the opposite direction as the ND2 force. We found that the presence of shear waves in domain 2 can influence and even determine the sign of the interaction force, which
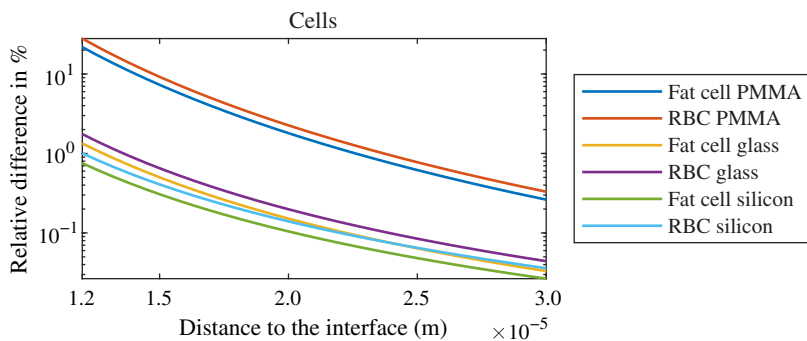

FIG. 8. The relative difference in percent for the acoustic radiation force between the ND2 model and the model with domain 2 included for cells (red blood cells and fat cells) placed close to experimentally relevant half-spaces (PMMA, glass, and silicon).
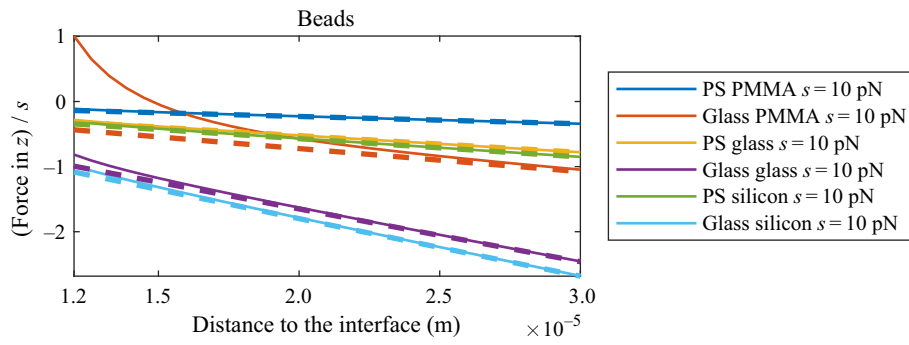
FIG. 9. The acoustic radiation force acting on standard beads (polystyrene and glass) placed close to a PMMA, glass, or silicon domain 2. The solid and dashed lines correspond to the models with and without domain 2, respectively. The acoustic force interactions lead to a sign inversion when a glass particle is placed close to a PMMA domain.

is investigated in Sec. V G. We speak of a sign inversion when the interaction force acts in the opposite direction as the ND2 force and is larger in amplitude. The increase or decrease in the interaction force and the occurrence of a sign inversion is the result of the complex interplay between the particle and domain material parameters. An example for this complex interplay is the case of an acoustically hard particle placed close to an acoustically soft domain 2, i.e., the LH LS case from Fig. 3. Equation (18) reveals that F^{GK} is positive, because the sign of $\sin(2kz)$ is negative, Φ is positive, and R is negative. This is shown by the dashed line in Fig. 3. However, the total acoustic radiation force, shown by the solid line, is negative if the particle is placed close to the interface. In this case the interaction force is negative and much larger in amplitude than the primary force, thus inducing the so-called sign inversion.

B. Limit cases

First, we investigate the simplest case: the soft and hard limit cases for the particle and domain 2. Our results for this setup are shown in Fig. 3. It can be observed that the interaction force F^I is quite weak for a hard particle placed close to a hard domain 2 (LH LH), for which the R_D remains below 5%. In the case of a soft particle placed close to a soft domain 2 (LS LS) the R_D can exceed 20% and decays very slowly with an increasing particle to wall distance. The interaction force F^I is strong if the particle and domain 2 are of different material models, i.e., for the combinations of soft particle hard domain 2 (LS LH) and

hard particle soft domain 2 (LH LS). In these cases, the interaction force F^I is larger in amplitude and of opposite sign with respect to F^{ND2}, thus inducing a sign change with respect to the model without domain 2.

C. General fluids and solids

In Fig. 4 we investigate the interaction of glass and soft fluidic particles with a rigid wall. The analytic results derived in Sec. II F are in good agreement with the finite element solution.

The case of solid particles close to a fluidic domain 2 is shown in Fig. 5. In the case of a hard or soft solid particle placed close to a hard domain 2 (SH FH and SS FH) we observe a R_D up to 10% for small separation distances of around 1.2 times the particle radius. The R_D for a soft (solid elastic) particle placed close to a soft (fluidic) domain 2 (SS FS) exceeds 80% for small separation distances. The interaction force F^I for a hard elastic particle placed close to a soft fluidic domain 2 (SH FS) is negative, which is in line with the the LH LS case from Fig. 3. In this case (SH FS), the interaction force even induces a sign change.

The complexity of the model can be further increased by allowing shear waves in domain 2. This is analyzed in Fig. 6, where we investigate the acoustic force interactions between a solid elastic particle and a solid elastic domain 2. In the case of soft-hard (SS SH) and hard-hard (SH SH) material combinations the R_D is between 20% and 30% if the particles are placed close to domain 2.

A strong positive interaction force F^I is observed for both cases with a soft solid domain 2 (SS SS or SH SS). In
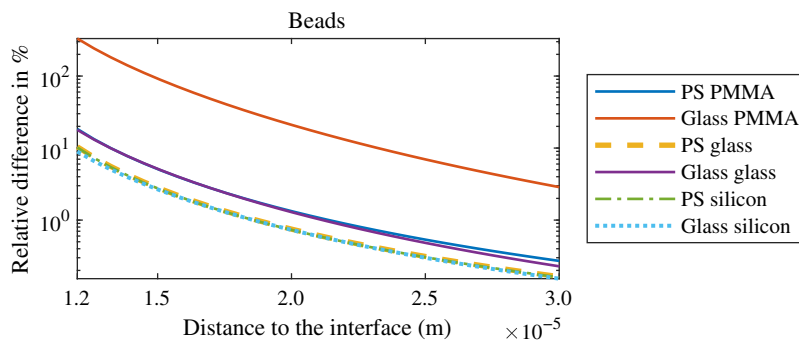

FIG. 10. The relative difference in percent for the acoustic radiation force between the ND2 model and the model with domain 2 included for standard beads (polystyrene and glass) placed close to a PMMA, glass, or silicon domain 2.
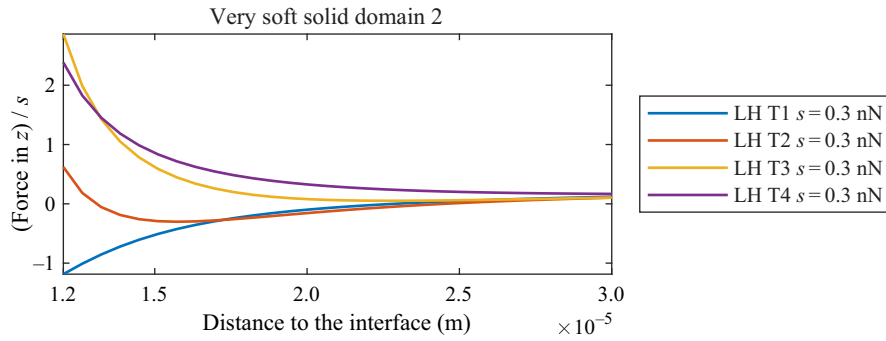
FIG. 11. The acoustic radiation force acting on an acoustically hard particle placed close to a very soft solid domain 2 (LH T). Here T1 is the softest material and T4 is the least soft material. It can be observed that changing the softness of the material will change the sign of the interaction force; for LH T1, the force is negative, as we expect from the SH FS and LH LS models. Increasing the stiffness of the domain 2 material will yield a positive acoustic interaction force (LH T3 and LH T4), which is in agreement with the SH SS model.

the case of a soft solid particle placed close to a soft solid domain 2 (SS SS) the interaction force F^I even induces a sign change. In the case of a soft fluidic domain 2 (SS FS or SH FS of Fig. 5), we observe a negative interaction force F^I. Thus, the F^I is of opposite sign in the SH SS setup with respect to the SH FS or LH LS setup, which is discussed in Secs. V F and V G.

D. Cells

The acoustic radiation force acting on cells (fat cells and red blood cells) close to PMMA, glass, and silicon is shown in Fig. 7. A closeup view is shown in Fig. 15. The biological cells in Fig. 7 are modeled as fluids. This assumption was previously used in scattering simulations by Hahn *et al.* [38] and Baasch *et al.* [39]. In Fig. 8 we show the R_D (in percent) for the cells close to PMMA, glass, and silicon interfaces, which corresponds to the

setup from Fig. 7. The R_D can exceed 20% for both types of cells if they are placed close to a PMMA domain 2. If the cells are placed close to a glass or silicon domain 2 the R_D is close to one percent.

E. Beads

The acoustic radiation force acting on solid elastic beads (polystyrene and glass) close to PMMA, glass, and silicon is shown in Fig. 9. The R_D for beads placed close to a PMMA, glass, or silicon domain 2 is shown in Fig. 10. The R_D is largest for a glass bead placed close to a PMMA domain 2 and even exceeds 100%. The other material combinations show a lower but still significant R_D of around 10 to 20% for small separation distances. Very close to interfaces the Gor'kov potential cannot thus be applied and more precise methods, such as numerical simulations, should be applied to calculate the acoustic radiation force.
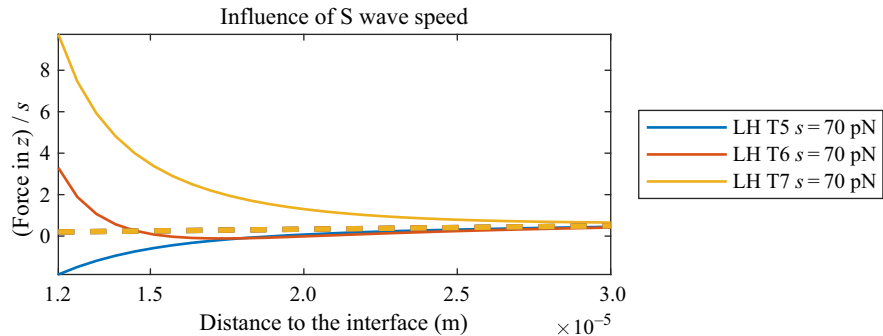

FIG. 12. The acoustic radiation force acting on an acoustically hard particle (LH) placed close to a shear soft solid elastic domain 2 (T5–T7). Here, T5 has the lowest and T7 has the highest S wave speed. The solid and dashed lines correspond to the models with and without domain 2, respectively. The dashed lines are the same for the three simulations and coincide. As shown in our analytical approximation in Sec. II E, the S wave speed inside domain 2 does not contribute to the ND2 force. If the S wave speed of the domain 2 material is low enough, i.e., for LH T5, then the solid half-space behaves as a fluid and the interaction force is negative. This effect is also observed in the SH FS case of Fig. 5. If the S wave speed is large enough, i.e., for LH T6 and LH T7, then the interaction force is positive, as observed in the SH SS case of Fig. 6.
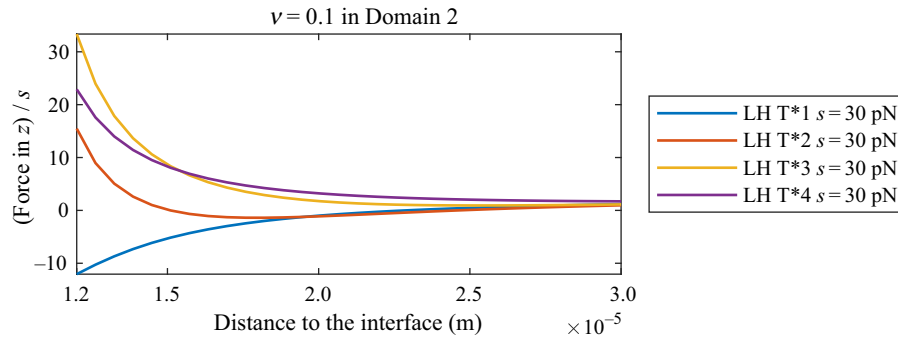
FIG. 13.   The acoustic radiation force acting on an acoustically hard particle placed close to a very soft solid domain 2 (LH T3). Here T*1 is the softest material and T*4 is the least soft material. It can be observed that changing the softness of the material will change the sign of the interaction force; for LH T*1, the force is negative, as we expect from the SH FS and LH LS models. Increasing the stiffness of the domain 2 material will yield a positive acoustic interaction force (LH T*4), which is in agreement with the SH SS model. The materials T* all have a Poisson ratio ν of 0.1.

F. Very soft materials in domain 2

In Fig. 11 we investigate the acoustic force interactions of a acoustically hard particle (LH) with very soft solid materials (T1–T4). The materials T1–T4 all have the same Poisson ratio ($0.\bar{3}$) as the ratio between the P and S wave speeds is constant. This Poisson ratio corresponds approximately to steel and is discussed in Sec. V H. It can be observed that in the limit of extremely soft solid materials (T1) the interaction force F^I is negative. This is in line with the limit case LH LS of Fig. 3. However, if the solid is sufficiently hard, i.e., has a high enough density and low enough compressibility (such as T3 and T4), then the acoustic interaction force F^I between the particle and domain 2 is positive, which is in line with the SH SS case of Fig. 6.

G. Influence of the S wave speed of domain 2

In Sec. V A we found that the interaction force F^I is positive for a hard particle placed close to a soft solid (SH SS case of Fig. 6). However, for a hard elastic particle placed close to a soft fluid, we found the interaction force F^I to be negative (SH FS case of Fig. 5). The main difference between the fluid and solid elastic material models are the S waves, which are present in the solid but not in the fluid. In Fig. 12 we investigate the acoustic radiation force acting on a hard particle (LH) placed close to a soft elastic half-space with low S wave speed. If the S wave speed of

the domain 2 material is low enough, i.e., for LH T5, then the solid half-space behaves as a fluid and the interaction force is negative. This effect is also observed in the SH FS case of Fig. 5. If the S wave speed is large enough, i.e., for LH T6 and LH T7, then the interaction force is positive, as observed in the SH SS case of Fig. 6.

H. Influence of the Poisson ratio

The materials T1–T4 all have the same R value and thus the same Poisson ratio of $\nu = 0.\bar{3}$. In order to see if the effect changes for another value of the Poisson ratio, we added Fig. 13. Here we used other materials denoted by T*, which all have a Poisson ratio of 0.1. The respective P and S wave speeds and densities for materials T*1–T*4 are given in Table III. Note that the Poisson ratio ν of a material can be expressed as a function of the ratio between the P and S wave speeds $q := c_p/c_s$ by

$$\nu = \frac{q^2 - 2}{2(q^2 - 1)}. \tag{27}$$

In Fig. 13 we can observe the same effect that is present in Fig. 11, i.e., there the interaction force F^I undergoes a sign change by going from soft solid materials to extremely soft solid materials in domain 2. This effect is not to be tied to the Poisson ratio of the T1–T4 materials.

TABLE III.   The table shows the material properties for the 0.1 Poisson ratio materials used in Fig. 13.

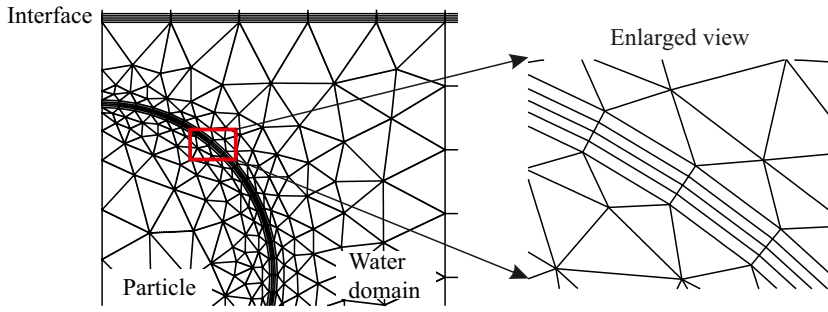| Material		Density	P wave speed	S wave speed	Poisson ratio ν
units	Tag	(kg m^{-3})	(m s^{-1})	(m s^{-1})	(TB)
Very soft solid 1*	T*1	50	50	$2/3 \times 50$	0.1
Very soft solid 2*	T*2	150	180	$2/3 \times 180$	0.1
Very soft solid 3*	T*3	200	240	$2/3 \times 240$	0.1
Very soft solid 4*	T*4	400	500	$2/3 \times 500$	0.1

FIG. 14. A closeup view of the mesh that we use to discretize the particle and its near surroundings. We use a refined rectangular mesh at the particle boundary (right panel) and at the interface between the water domain and the half-space. The near surroundings of the particle are discretized using a triangular mesh (left panel). Further away (not shown in the panels), we use a rectangular mesh for efficient meshing.

VI. CONCLUSION

In several cases we observe a strong acoustic interaction force F^I. This effect is more pronounced if the particle is placed close to the interface. For particles placed far enough from the interface, we find the acoustic interaction force F^I to be negligible. We find a strong acoustic interaction force F^I for very hard particles placed close to a soft domain 2, such as LH LS (Fig. 3), SH SS (Fig. 6) and SH FS (Fig. 5), or even in the experimentally relevant setup of a glass particle placed close to a PMMA domain 2 (Fig. 9). For the LH LS (Fig. 3), LS LH (Fig. 3), SH FS (Fig. 5), SS SS (Fig. 6), and glass PMMA (Fig. 9) cases the interaction force is of higher amplitude and opposite sign than the force without domain 2 and induces a sign change in the acoustic radiation force if the particle is placed close enough to the interface.

We find that, for hard particles (LH, SH) placed close to a soft domain 2, the sign of the interaction force F^I depends on the softness and the S wave speed inside domain 2. If the material of domain 2 is soft enough and has small enough S wave speed then we find the interaction force to be negative, as shown in the LH LS (Fig. 3), SH FS (Fig. 5), LH T1 (Fig. 11), LH T5 (Fig. 12), and LH T*4 (Fig. 13) setups.

In the practically relevant cases of Figs. 7 and 9 the R_D is small only for cells placed close to a silicon or glass domain 2, in all other cases the R_D exceeds 10% close

to domain 2. In the case of a glass particle placed close to a PMMA domain 2, the R_D even exceeds 100% and the interaction force F^I is strong enough to induce a sign inversion.

Gor'kov's formulation does not give reliable results for the acoustic radiation force acting on particles close to a half-space and more accurate models, i.e., numerical models, are needed to correctly assess the acting acoustic force. In experimental works such as the acoustic force spectroscopy [22,23] and the acoustic tweezing cytometry [24] good care needs to be taken regarding the material combinations and the modeling, such that the acoustic interactions are minimized or modeled correctly.

APPENDIX A: CLOSEUP OF THE MESH

A view of our mesh close to the particle is shown in Fig. 14. We use a smaller rectangular mesh close at the particle boundary (right panel) and the interface between the half-spaces. The near surroundings of the particle, which are shown in the left panel, are discretized using a triangular mesh. Further away, which is not shown in the Fig. 14, we use rectangular mesh elements.

APPENDIX B: CLOSEUP OF FIG. 7
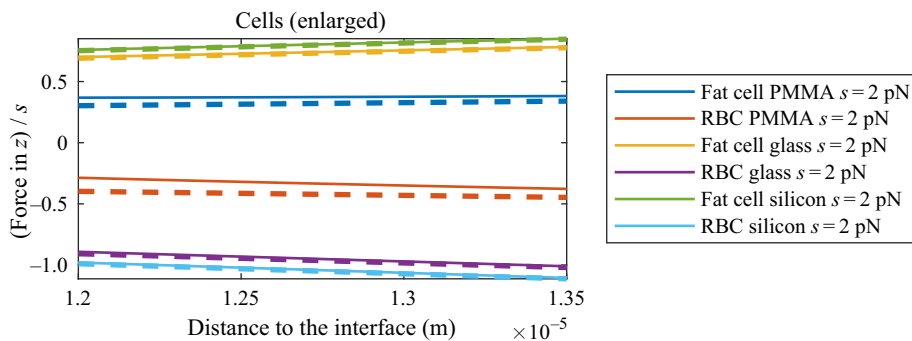
A closeup view of Fig. 7 is shown in Fig. 15.

FIG. 15. A closeup view of Fig. 8. The solid and dashed lines correspond to the models with and without domain 2, respectively.

[1] S. D. Howkins, Measurements of the resonant frequency of a bubble near a rigid boundary, J. Acoust. Soc. Am. **37**, 504 (1965).

[2] A. Shima, K. Takayama, Y. Tomita, and N. Miura, An experimental study on effects of a solid wall on the motion of bubbles and shock waves in bubble collapse, Acta Acust. united Ac. **48**, 293 (1981).

[3] Shukui Zhao, Katherine W. Ferrara, and Paul A. Dayton, Asymmetric oscillation of adherent targeted ultrasound contrast agents, Appl. Phys. Lett. **87**, 134103 (2005).

[4] Shukui Zhao, Dustin E. Kruse, Katherine W. Ferrara, and Paul A. Dayton, Acoustic response from adherent targeted contrast agents, J. Acoust. Soc. Am. **120**, 63 (2006).

[5] Edward M. B. Payne, Suhith J. Illesinghe, Andrew Ooi, and Richard Manasseh, Symmetric mode resonance of bubbles attached to a rigid boundary, J. Acoust. Soc. Am. **118**, 2841 (2005).

[6] V. Garbin, D. Cojoc, Enrico Ferrari, E. Di Fabrizio, M. L. J. Overvelde, S. M. Van Der Meer, N. De Jong, Detlef Lohse, and Michel Versluis, Changes in microbubble dynamics near a boundary revealed by combined optical microma-nipulation and high-speed imaging, Appl. Phys. Lett. **90**, 114103 (2007).

[7] Alexander A. Doinikov, Leila Aired, and Ayache Bouakaz, in *2010 IEEE Ultrasonics Symposium (IUS)* (IEEE, San Diego, California, USA, 2010), p. 1133.

[8] A. Shima and Y. Tomita, The behavior of a spherical bub-ble near a solid wall in a compressible liquid, Arch. Appl. Mech. **51**, 243 (1981).

[9] A. Shima, Studies on bubble dynamics, Shock Waves **7**, 33 (1997).

[10] Alexander A. Doinikov, Shukui Zhao, and Paul A. Day-ton, Modeling of the acoustic response from contrast agent microbubbles near a rigid wall, Ultrasonics **49**, 195 (2009).

[11] Jingtao Wang and Jurg Dual, Theoretical and numerical cal-culation of the acoustic radiation force acting on a circular rigid cylinder near a flat wall in a standing wave excitation in an ideal fluid, Ultrasonics **52**, 325 (2012).

[12] Yupei Qiao, Xiaofeng Zhang, and Guangbin Zhang, Acous-tic radiation force on a fluid cylindrical particle immersed in water near an impedance boundary, J. Acoust. Soc. Am. **141**, 4633 (2017).

[13] G. C. Gaunaurd and H. Huang, Acoustic scattering by a spherical body near a plane boundary, J. Acoust. Soc. Am. **96**, 2526 (1994).

[14] Alexander A. Doinikov, Leila Aired, and Ayache Bouakaz, Dynamics of a contrast agent microbubble attached to an elastic wall, IEEE Trans. Med. Imag. **31**, 654 (2012).

[15] Alexander A. Doinikov, Leila Aired, and Ayache Bouakaz, Acoustic response from a bubble pulsating near a fluid layer of finite density and thickness, J. Acoust. Soc. Am. **129**, 616 (2011).

[16] Alexander A. Doinikov, Leila Aired, and Ayache Bouakaz, Acoustic scattering from a contrast agent microbubble near an elastic wall of finite thickness, Phys. Med. Biol. **56**, 6951 (2011).

[17] Alexander A. Doinikov and Ayache Bouakaz, Ultrasoni-cally induced dynamics of a contrast agent microbubble between two parallel elastic walls, Phys. Med. Biol. **58**, 6797 (2013).

[18] Peter Glynne-Jones, Puja P. Mishra, Rosemary J. Boltryk, and Martyn Hill, Efficient finite element modeling of radia-tion forces on elastic particles of arbitrary size and geome-try, J. Acoust. Soc. Am. **133**, 1885 (2013).

[19] Jingtao Wang and Jurg Dual, Numerical simulations for the time-averaged acoustic forces acting on rigid cylinders in ideal and viscous fluids, J. Phys. A **42**, 285502 (2009).

[20] Kotaro Sato, Yukio Tomita, and Akira Shima, Numeri-cal analysis of a gas bubble near a rigid boundary in an oscillatory pressure field, J. Acoust. Soc. Am. **95**, 2416 (1994).

[21] Q. X. Wang and K. Manmi, Three dimensional microbubble dynamics near a wall subject to high intensity ultrasound, Phys. Fluids **26**, 032104 (2014).

[22] Gerrit Sitters, Douwe Kamsma, Gregor Thalhammer, Monika Ritsch-Marte, Erwin J. G. Peterman, and Gijs J. L. Wuite, Acoustic force spectroscopy, Nat. Methods **12**, 47 (2014).

[23] Douwe Kamsma, Ramon Creyghton, Gerrit Sitters, Gijs J. L. Wuite, and Erwin J. G. Peterman, Tuning the music: Acoustic force spectroscopy (afs) 2.0, Methods **105**, 26 (2016).

[24] Zhenzhen Fan, Yubing Sun, Di Chen, Donald Tay, Weiqiang Chen, Cheri X. Deng, and Jianping Fu, Acous-tic tweezing cytometry for live-cell subcellular modulation of intracellular cytoskeleton contractility, Sci. Rep. **3**, 2176 (2013).

[25] L. P. Gor'Kov, in *Soviet Physics Doklady* (1962), Vol. 6, p. 773.

[26] L. D. Landau, Em lifshitz, fluid mechanics, Course Theor. Phys. **6**, 253 (1987).

[27] Alexander A. Doinikov, Acoustic radiation interparticle forces in a compressible fluid, J. Fluid Mech. **444**, 1 (2001).

[28] Henrik Bruus, Acoustofluidics 7: The acoustic radiation force on small particles, Lab Chip **12**, 1014 (2012).

[29] David T. Blackstock, Fundamentals of physical acoustics (Wiley interscience, 2001), p. 108.

[30] W. Maurice Ewing, Wenceslas S. Jardetzky, Frank Press, and Arthur Beiser, *Elastic Waves in Layered Media* (Graw Hill Book Company, Inc., 1957).

[31] Jonas T. Karlsen and Henrik Bruus, Forces acting on a small particle in an acoustical field in a thermoviscous fluid, Phys. Rev. E **92**, 043010 (2015).

[32] Mikkel Settnes and Henrik Bruus, Forces acting on a small particle in an acoustical field in a viscous fluid, Phys. Rev. E **85**, 016327 (2012).

[33] Glauber T. Silva and Henrik Bruus, Acoustic interaction forces between small particles in an ideal fluid, Phys. Rev. E **90**, 063007 (2014).

[34] Alan R. Selfridge, Approximate material properties in isotropic materials, IEEE Trans. Sonics Ultrason. **32**, 381 (1985).

[35] K. K. Shung III, B. A. Krisko, and J. O. Ballard, Acous-tic measurement of erythrocyte compressibility, J. Acoust. Soc. Am. **72**, 1364 (1982).

[36] Deny Hartono, Yang Liu, Pei Lin Tan, Xin Yi Sherlene Then, Lin-Yue Lanry Yung, and Kian-Meng Lim, On-chip measurements of cell compressibility via acoustic radiation, Lab Chip **11**, 4072 (2011).

[37] A. H. Frucht, Die schallgeschwindigkeit in menschlichen und tierischen geweben, Z. Gesampte Exp. Med. **120**, 526 (1953).

[38] Philipp Hahn, Ivo Leibacher, Thierry Baasch, and Jurg Dual, Numerical simulation of acoustofluidic manipulation by radiation forces and acoustic streaming for complex particles, Lab Chip **15**, 4302 (2015).

[39] Thierry Baasch and Jürg Dual, Acoustofluidic particle dynamics: Beyond the Rayleigh limit, J. Acoust. Soc. Am. **143**, 509 (2018).